ACS OMEGA

http://pubs.acs.org/journal/acsodf

Article

Numerical Simulation Study on the Flow Field and Separation Efficiency by Built-In Twisted Tape in the Hydrocyclone

Yongchao Rao, Yong Hu, Shuli Wang,* Shuhua Zhao, and Shidong Zhou

Cite This: *ACS Omega* 2023, 8, 26301−26316

Read Online

ACCESS | Metrics & More | Article Recommendations

ABSTRACT: Aiming at the separation of mud and sand in natural gas hydrate, for the designed built-in twisted tape hydrocyclone, the numerical simulation method was used to study the effects of different types of built-in twisted tape and operating conditions on the internal flow field of the hydrocyclone, separation efficiency, and influence of hydrate particle size distribution. The research results show that the built-in twisted tape has the same swirling direction as the hydrocyclone, which is beneficial to improving the swirling intensity, and the ability to carry and separate solid particles is obviously enhanced. The built-in twisted tape hydrocyclone with a length of 300 mm has better separation efficiency and internal flow field stability. By changing the conditions of the inlet velocity and the initial concentration of hydrate particles, the comparison shows that when the inlet velocity is 8 m/s, the volume of mud and sand is 25%, the initial concentration of hydrate particles is 15%, and the built-in tape is 300 mm long. The tape hydrocyclone has the best separation efficiency. Compared with the basic hydrocyclone, the built-in twisted tape hydrocyclone with a length of 300 mm increases the separation efficiency of mud and sand by 7.49%, while the pressure drop only increases by 2.67%, showing the superiority of the built-in twisted tape structure.

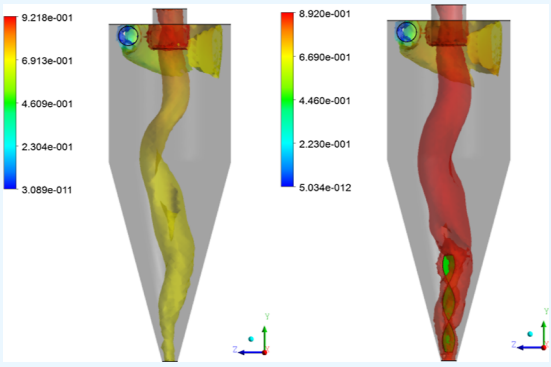

1. INTRODUCTION

Global natural gas hydrates are mainly distributed in the polar regions and deep ocean areas, and marine hydrate resources account for more than 95% of the total hydrate resources.[1] At present, marine diagenetic gas hydrate resources can be exploited by changing phase balance methods such as depressurization, heat injection, agent injection, and gas replacement. For marine non-diagenetic gas hydrate resources, Zhou et al.[2] proposed deep-water and shallow non-diagenetic natural gas. Hydrate solid-state fluidization mining technology successfully completed the deep-water shallow non-diagenetic gas hydrate solid-state fluidization operation in the Shenhu area of the South China Sea in 2017, marking that the hydrate solid-state fluidization mining method can solve the problem of non-diagenetic hydrate resource mining.[3] However, in the solid-state fluidized exploitation of marine hydrates, there are many problems in the pre-separation technology of hydrate mud and sand and the pipeline transportation technology of hydrate slurry, and these problems have a great impact on non-diagenetic hydrate resource mining.

In view of the fact that there are few studies on the separation of hydrate-sand-sand mixed slurry and the transportation of marine hydrate slurry under swirl flow in the solid-state fluidized mining of marine hydrates, it is urgent to carry out the selection and optimization of underwater pre-separation equipment and the swirl flow pipeline transportation of hydrate slurry. Numerical simulation research plays an important role in marine hydrate development and research and has become a must-do project before and after hydrate field test research.[4] Before the trial mining research, through the simulation test, the operation of the target hydrate in the equipment and the changes of other parameters should be investigated, the process equipment should be optimized, and the test results should be preliminarily judged so as to achieve the purpose of technical improvement. Simulation research on the underwater pre-separation and transportation of marine hydrate is an important way to promote the industrial application of natural gas hydrate.

In recent years, with the deepening of the research on hydrocyclones by experts and scholars, the hydrocyclone and its related technologies have been developed rapidly. The hydrocyclone has a simple internal structure, a small volume, high separation efficiency, a long service life, and convenient maintenance in later periods. It is especially suitable for the engineering process that is not conducive to frequent replacement of separation equipment, so it has become common equipment for underwater separation operations.[5] By changing

Received: April 20, 2023
Accepted: June 29, 2023
Published: July 13, 2023

https://doi.org/10.1021/acsomega.3c02549
ACS Omega 2023, 8, 26301−26316

the structure and optimizing the operating conditions, it can be adapted to the separation of different types of minerals. It is very suitable equipment for underwater pre-separation of marine hydrate solid-state fluidization mining. Due to the great difference in the density of the two materials in the hydrate-slurry mixed slurry, in the separation process, quickly gathering and discharging light hydrate particles from the overflow is the key to affecting the separation efficiency. However, the structure of the hydrocyclone is simple, and the internal flow field is relatively complicated. It is difficult for the experimental device to measure materials with opaque and high concentration.[6] With the development of computational fluids, the numerical simulation method has become the mainstream method to study the performance of hydrocyclones, and the research on hydrocyclones whose structure will be improved by the numerical simulation method has also been affirmed by the industry. Xu et al.[7] verified the accuracy of using the Reynolds stress model to simulate the particle motion of the hydrocyclone by comparing it with the particle motion trajectories in the particle image velocity (PIV) and used the Reynolds stress model to simulate the internal flow field of the hydrocyclone. The results show that the simulated flow field is in good agreement with the actual flow field, which further verifies the accuracy and practicability of the numerical simulation. Baker et al.[8] proposed the structural form of the reverse flow hydrocyclone and analyzed it numerically. The results show that adding a hydrocyclone to the overflow port inside the hydrocyclone solves the problem that the separated liquid with a small density difference is discharged from the same outlet at the same time during the three-phase separation process. The device is suitable for the separation of underground mineral deposits. Westra et al.[9] proposed a bushed hydrocyclone structure. The main external components of the conventional hydrocyclone, such as the barrel and the cone, are all fixed parts, so the maximum value of the rotation speed near the wall is limited by the structure of the hydrocyclone. The lower cone part of the hydrocyclone is equipped with an inner ring bearing structure, and the upper cylinder part is equipped with an outer ring bearing. During operation, the lower cone section rotates with the movement of the cylinder section, which increases the rotation speed value. When the material moves at high speed in the hydrocyclone, the rotation and swirl speed of the cone section make the separated material obtain a larger centrifugal force, thereby improving the separation efficiency. Zhao et al.[10] designed a hydrocyclone with a built-in thimble in the bottom flow port. The research shows that the built-in thimble is installed at the sand settling port, and the lower cone part contains substances that are not completely separated from oil and water. The presence of the built-in thimble makes the oil phase particles gather at the tip of the thimble in the inner swirl zone. Presence to make the oil phase more easily drained from the overflow. Under different inlet flow rates, the built-in thimble hydrocyclone improves the separation efficiency by more than 10% and reduces the pressure drop by 50% compared with the ordinary hydrocyclone. Gomez et al.[11] designed a helical vane hydrocyclone in which a hydrocyclone is installed with helical vanes at the overflow. The results show that the tangential velocity increases when the oil−water mixture enters the position of the helical blade from the feed port. By increasing the tangential velocity, the swirl intensity can be increased, thereby increasing the swirl intensity in the oil−water mixture. When the oil−water mixture moves into the cone section, the rotation radius of the oil−water mixture will decrease due to the limitations of the cone wall. The rotation radius is inversely proportional to the swirl intensity. The swirl blade and the cone part enhance the swirl flow, and there is a density difference in the oil−water mixture, which improves the oil−water separation efficiency. However, the increased resistance and turbulent kinetic energy pulsation on the surface of the helical blade will lead to the separation of the boundary layer, thus affecting the separation efficiency. When setting the twisted tape in the hydrocyclone to enhance the strength of the swirl, it is necessary to avoiding the length of the twisted tape be too long. Shang et al.[12] designed a new type of slotted helical vane hydrocyclone and used FLUENT fluid software to optimize the separation efficiency, pressure field, and oil phase distribution for numerical simulation. The results show that compared with the hydrocyclone of the same size, the optimized slot hydrocyclone has a separation efficiency of 93.7%, the internal velocity field is circumferentially symmetrical, the internal flow field is more stable, and the oil content of the underflow port is reduced. Zhao et al.[13] designed an inner cone hydrocyclone, and the results show that the inner cone structure provides a more stable flow field for the separated phases, which is beneficial to the radially separated gas accumulation and the formation of larger bubbles. It also pushes the air bubbles upwards to improve the gas−liquid separation performance. At the same time, Zhao et al.[14] studied the effect of inner cone diameter on the degassing and desander hydrocyclones. The results show that the diameter of the inner cone has a significant effect on the separation efficiency. The solid phase separation efficiency of the separator with an inner cone diameter of 30 mm, an inlet flow rate of 1.1 m^3/h, and an overflow split ratio of 60% is as high as 85.8%. Chen et al.[15] designed a hydrocyclone suitable for the separation of hydrate mud−sand mixed slurry. By changing the cone angle, inlet flow rate, mixed slurry volume fraction, and particle size of the hydrocyclone, changes can be made to the separation efficiency of hydrocyclones. The results show that in the hydrocyclone with a cone angle of 15°, the particle size is 50−70 μm, the inlet flow rate is 7 m/s, and the volume fraction of mud and sand is about 25%; the separation efficiency is the highest. At the same time, Chen proposed a double-cone-inner-cone hydrocyclone and studied the effect of particle size, cone angle combination, and inlet pressure on the separation efficiency of solid particles and natural gas. The results show that the separation efficiency is best when the particle size of solid particles is 50−90 μm, the diameter of natural gas bubbles is 400−800 μm, the inlet pressure is 4.3−7.3 MPa, and the optimal cone angle combination of cone segment and inner cone is 10 and 5°. However, Qiu et al.[16] only designed and optimized the structure of the separator, and the results showed that with the increase of the diameter of the overflow port, the cone angle, the length of the cylindrical section, and the diameter of the underflow port, the separation efficiency first increased, and then the hydrate recovery efficiency was as high as 98.5% when the structure was optimized by the orthogonal method. Considering the recovery of natural gas hydrate to the greatest extent, the orthogonal test method is better for optimizing the structural parameters of the purification separator, and the bottom flow port should be considered. The research of Liu and Wang[17] showed that the structure improvement and the design of the new hydrocyclone will improve the separation efficiency, but the improvement potential is limited, and the operating parameters need to be optimized to achieve the highest separation efficiency. Wang's research group has also done some research and exploration into the formation and separation of hydrate.[18−20] The above-

https://doi.org/10.1021/acsomega.3c02549
ACS Omega 2023, 8, 26301−26316

mentioned relevant experts and scholars have conducted numerical simulation and experimental verification studies on hydrocyclones, but there are few studies on the separation law of hydrate particles, the hydrocyclone has a single form and structure, and there is a big gap in the separation efficiency of different occasions.

Lafond[21] carried out experiments on the flow characteristics of hydrate particles, focusing on the effects of hydrate volume fraction and fluid conversion velocity on the movement of hydrate particles in the pipeline, which can provide an experimental reference for the movement law of hydrate particles and control hydrate slurry blockage. Majid et al.[22] carried out experiments on hydrate flow characteristics with the high-pressure loop of Tulsa University as the experimental platform to solve the problem of hydrate flow guarantee in the pipeline. The experimental results show that the liquid velocity and water content have a great influence on the hydrate flow in the pipeline. In addition, the viscosity change in the hydrate formation process also has a great impact on the hydrate flow. The viscosity is greater, and the fluidity is worse. Yongchao et al.[23,24] studied the flow characteristics of gas−liquid two-phase spiral flow and hydrate formation characteristics based on spiral flow. Ding et al.[25] carried out research on hydrate flow and pipe plugging characteristics in oil and gas gathering and transmission pipelines. Based on the experimental results, the hydrate deposition and pipe plugging mechanisms under different hydrate slurry flow patterns are obtained, and the method of quantitative calculation of deposition is deduced. The above experts and scholars have studied the flow and deposition laws of hydrate particles and preliminarily grasped the doom and fall law of hydrate particles, but there are few studies on the movement laws of hydrate particles in the hydrocyclone.

In general, simulation research on the underwater pre-separation and transportation of marine hydrate is an important way to promote the industrial application of natural gas hydrate. Therefore, a hydrocyclone should be developed and designed which is more suitable for the separation of hydrate after mining, and the separation characteristics of hydrate particles need to be studied. The research work in this paper is to provide theoretical support for the development of hydrate solid-state fluidization mining technology in the future on how to improve the hydrocyclone separation efficiency of mud and sand in hydrate and the transportation technology to improve the hydrate carrying capacity.

2. NUMERICAL SIMULATION METHOD

2.1. Structure and Size. According to relevant empirical formulas, the cylinder height (h_1) is 285 mm, the cylinder diameter (d_1) is 250 mm, the conical cylinder height (h_2) is 463 mm, and the cone angle (θ) is 15°. The top of the cylinder is provided with an overflow port, and the side wall is provided with a feed port. The overflow mouth diameter (d_2) is 70 mm, the total length of the overflow pipe (l_1) is 85 mm, which stretches into the depth of the cylinder body (l_2) of 65 mm, the inlet diameter (d_3) is 40 mm, and the length (l_3) is 50 mm. The bottom of the conical cylinder is provided with a sand-settling mouth, and the diameter (d_4) is 30 mm. They are shown in Figure 1.

The twist tape has the effect of forcing rotation, which can improve the strength of the cyclone. At the same time, it is placed at the sand-settling mouth of the hydrocyclone, occupying the position of the air column and forcing the air column to move upward, which makes it easier to increase the

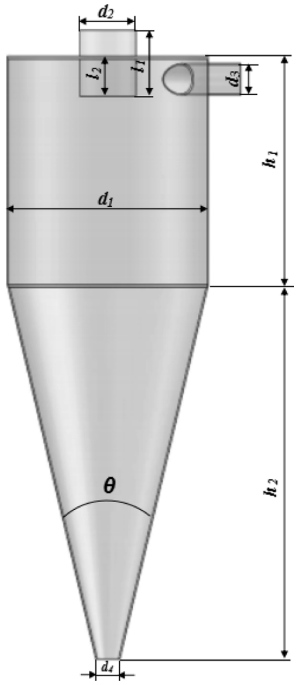

Figure 1. Basic hydrocyclone structure sketch.

upward thrust on the gas and hydrate particles, and it has a certain effect on eliminating the air column generated at the bottom. The twisted tape with a twist rate of $Y = 6.2$ $(Y = H/D)$ was adopted. In the internal twisted tape hydrocyclone, four twisted tapes were chosen with the same twist rate Y and different lengths of L_i and one twisted tape had a reduced diameter of 0.5 mm. Figure 2 shows the structure of a twisted tape.

The built-in twisted tape hydrocyclone has the same structure as the foundation cyclone, and the built-in twist-tape is fixed by a bracket at the bottom of the cone. It can be used to enhance the

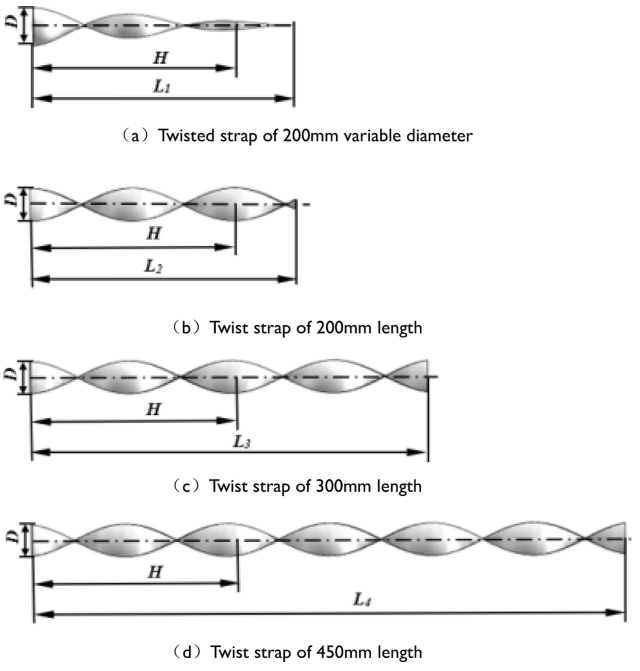

Figure 2. Structural sketch of built-in twisted tape.

https://doi.org/10.1021/acsomega.3c02549
ACS Omega 2023, 8, 26301−26316

strength of swirl, prolong the separation time, and improve the separation efficiency of mud and sand. At the same time, in order to avoid the removal of fine sand from the bottom flow orifice by the twisted tape, the distance between the twisted tape and the settling sand orifice is 15 mm, and two fixed supports are installed at the position of the twisted tape and fixed at the position of the cone, so the twisted tape is not easy to distort and offset during the separation process.

2.2. Working Condition Setting. The performance of the basic hydrocyclone and the built-in 300 mm long twisted tape hydrocyclone were compared by changing the operating conditions. Under the premise that the initial concentration of mud and sand particles is 25% and the particle size of mud and sand particles remains unchanged by changing the initial concentration of hydrate and the inlet flow rate conditions, the effect of a basic hydrocyclone and a built-in twisted tape hydrocyclone on mud and sand separation efficiency and hydration is studied. The 20 groups of working conditions are simulated, and the designed working condition parameters are shown in Table 1.

Table 1. Simulated Condition Parameter Table

working condition	flow velocity V_0 (m/s)	hydrate volume fraction α(%)	with/without twist tape
case 1	7	10	have
case 2	7	15	have
case 3	7	20	have
case 4	7	30	have
case 5	7	10	nothing
case 6	7	15	nothing
case 7	7	20	nothing
case 8	7	30	nothing
case 9	5	15	have
case 10	6	15	have
case 11	7	15	have
case 12	8	15	have
case 13	9	15	have
case 14	10	15	have
case 15	5	15	nothing
case 16	6	15	nothing
case17	7	15	nothing
case 18	8	15	nothing
case 19	9	15	nothing
case 20	10	15	nothing

2.3. Physical Model. *2.3.1. Meshing.* The hydrocyclones are all divided by unstructured meshes, as shown in Figure 3. In the pipeline swirl flow, the short twisted tape is selected as the spinner. The short twisted tape spinner adopts an unstructured mesh, as shown in Figure 4a and is assembled with a 2 m long structured mesh pipeline. Figure 4b.

2.3.2. Grid Independence Verification. The twisted tape and the settling mouth are occupied in the position of the air column, which prevents the production of the air column or forces it to move up the direction of the overflow port. A twisted tape is arranged at the settling port of the hydrocyclone, which can enhance the internal swirl effect at the beginning.

For the simulation of hydrocyclone separation, the grid number of the hydrocyclone is 135,105, the grid number of the built-in twisted tape hydrocyclone with a length of 200 mm is 675,455, and the grid of the built-in twisted tape hydrocyclone with a length of 300 mm is 675,455. The number of grids is

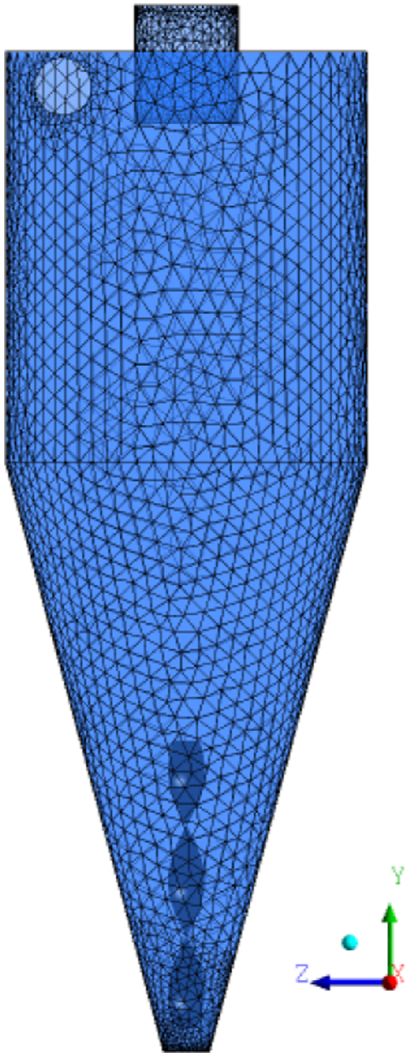

Figure 3. Mesh generation of the built-in twisted tape hydrocyclone.

739,824, the grid number of the built-in twisted tape hydrocyclone with a length of 450 mm is 794,608, and the grid number of the built-in variable diameter twisted tape hydrocyclone with a length of 200 mm is 749,790.

For the simulation of pipeline helical flow transportation, the total number of grids of the short twist tape spinner is 486,360, and the total number of grids of the ordinary horizontal pipeline of the control group is 234,566. The mesh quality is above 0.8. The number of grids simulated in the above two aspects has been verified by grid independence and meets the requirements of grid independence.

2.3.3. Boundary Conditions. In the simulation of the hydrocyclone separator, the inlet velocity (velocity inlet) is set for the material of the hydrocyclone. In the pre-separation of seabed hydrate, the inlet port is a solid−liquid two-phase of mud sand, seawater, and hydrate. The overflow and underflow port selections are free outflow with no wall slippage. In the aspect of pipeline helical flow simulation, the short-twisted tape spinner of the pipeline adopts the Cartesian coordinate system for calculation, and the coordinate origin is set at the center of the pipeline inlet surface. The flow medium in the pipe is seawater and hydrate particles, and the flow medium is specified to move in the positive direction of the Y axis. The inlet of the pipe adopts velocity-inlet, the outlet adopts natural outflow, and

https://doi.org/10.1021/acsomega.3c02549
ACS Omega 2023, 8, 26301−26316

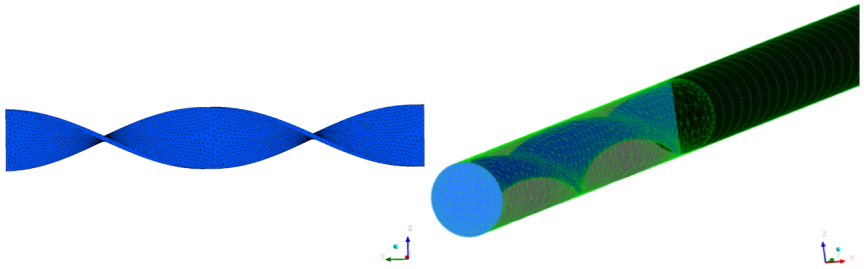

（a）Short tape swirl generator （b）Pipeline length of 2 m

Figure 4. Mesh generation of a short tape swirl generator in pipeline.

the pipe wall has no slippage. The gravity is along the negative *z*-axis, and the gravity is 9.81 m/s^2. Adopt SIMPLEC-based velocity-pressure coupling algorithm. Momentum and turbulent dissipation rates are both in a second-order upwind discrete format. The convergence accuracy is set to 10^{-5}, the time step is 0.00125 s, and the calculation is stopped when the convergence accuracy requirements are met.

2.3.4. Initial Conditions. According to the actual situation, refer to the operating conditions of solid-state fluidized mining of hydrate in deep water and shallow layers.[26] The flowing medium is determined to be seawater, natural gas hydrate, and silt, and the multiphase flow model is used to simulate the movement of the gas hydrate silt-sand mixed slurry in the hydrocyclone. The gas hydrate particle size is 60 μm solid particles, and the mud sand particle size is 90 μm solid particles. Table 2 shows the medium parameters of gas hydrate mud−sand mixed slurry.

Table 2. Medium Parameters of Marine Gas Hydrate Slurry

material	density/(kg/m^3)	density/[kg/(m·s)]
seawater	1025	0.0017
marine natural gas hydrate	650	1.30×10^{-5}
loam	2600	1.72×10^{-5}

2.4. Mathematical Model. *2.4.1. Governing Equation.* Since the volume ratio of the particle phase is greater than 10%, the discrete phase of the particle phase can be regarded as a continuous phase. The multiphase flow model adopts the Euler-Eulerian two-fluid model. The governing equations for the liquid phase include the momentum equation and the continuity equation, respectively. The formulae 1 and 2 are shown in ref 27

$$\frac{\partial(\rho_i\alpha_i)}{\partial t} + \nabla\cdot(\rho_i\alpha_i\boldsymbol{v}_i) = 0 \tag{1}$$

$$\frac{\partial(\alpha_i\rho_i\boldsymbol{v}_i)}{\partial t} + \nabla\cdot(\rho_i\alpha_i\boldsymbol{v}_i\boldsymbol{v}_i) = -\alpha_i\nabla p + \nabla\cdot\boldsymbol{\tau}_i + \alpha_i\rho_i g + M_i \tag{2}$$

where i is the water phase or hydrate particle phase; ρ is the density, kg/m^3; v is the velocity vector, m/s; p is the pressure, Pa; τ_i is the stress tensor, Pa; and M_i is the interphase momentum exchange term, kg/(m·s)^2. In the interaction between the fluid and the solid in the simulation study, momentum exchange occurs. When the momentum M_i exchange occurs, the interphase drag force M_{di} and the turbulent diffusion force M_{ti} are taken into account in the momentum exchange, and t_i establishes the interphase force model to closed multiphase flow model, such as formula 3.

$$M_i = M_{di} + M_{ti} = k_{ls}\left(\boldsymbol{v}_r - \frac{\mu_t}{\rho_m\alpha_s\sigma_d}\nabla\alpha_l\right) \tag{3}$$

where $\boldsymbol{v}_r$ is the relative velocity between phases, m/s; μ_t is the turbulent viscosity, kg/(m·s); ρ_m is the density of the mixed phase; σ_d is the diffusion coefficient; α_s is the volume fraction of hydrate particles; α_l is the water phase volume fraction; and k_{ls} is the momentum transfer coefficient. Since the hydrate slurry is formed by mixing water and hydrate particles, the drag force has a great influence on the crushing and aggregation of the medium. For the case where the drag force is considered, the hydrate particles are formed by water and hydrate particles, the model is suitable for sparse phase flow with a volume fraction of the secondary phase significantly lower than that of the main phase, and the liquid−solid drag force adopts the Wen−Yu model,[28] and k_{ls} is the momentum transfer coefficient.

2.4.2. Turbulence Equation of Motion. When the Reynolds stress model needs to be used in the turbulence model, the Reynolds stress equation of the RSM model[29] (4) is as follows

$$\frac{\partial}{\partial t}(\rho\overline{u_iu_j}) + \frac{\partial}{\partial x_k}(\rho u_k\overline{u_iu_j}) = D_{ij} + P_{ij} + \Phi_{ij} - \varepsilon_{ij} \tag{4}$$

The right side of the equation is arranged in order as the stress diffusion term, the stress generation term, the stress change term, and the dissipation term. The change term in the third term of the right equation is necessary, which can explain the change process provided by the Reynolds stress.[30] Due to the strong rotating flow in the solid−liquid hydrocyclone, RSM is used as the turbulent flow model in this paper. This model eliminates the defect of turbulent viscosity isotropy in the eddy-viscosity assumption and predicts the motion behavior of the mud−sand hydrate mixed particle in the hydrocyclone more effectively.

2.4.3. Group Balance Model. In the system of multiphase flow, these discrete phases carry out material exchange and transfer, resulting in nucleation, growth, fragmentation, and aggregation. These particle groups are then represented by the number density function.[31] This paper assumes that the generation and decomposition of hydrate particles are not considered, and its population balance equation[18] can be expressed as formula 5. The population balance model was first used to describe the dynamic balance of population and was subsequently applied to the industrial field to describe the particle size distribution of solid

https://doi.org/10.1021/acsomega.3c02549
ACS Omega 2023, 8, 26301−26316

$$\frac{dn(L,t)}{\partial t} = \frac{1}{2}\int_0^L a\beta(L-L',L')n(L-L',t)dL' - \int_0^\infty a\beta(L,L')n(L',t)n(L,t)dL' + \int_L^\infty b(L|L')S(L')n(L',t)dL' - S(L)n(L,t) \quad (5)$$

where $n(L,t)$ is the number density of hydrate particles with particle size L at time t, $1/m^3$; $\beta(L-L',L')$ is the collision frequency of $L-L'$ and L' two hydrate particles, m^3/s; a is the merging efficiency of two hydrate particles after collision; $S(L')$ is the L' crushing frequency of hydrate particles, $1/s$; and then, $b(L/L')$ is the probability that hydrate particles with particle size are generated after the hydrate particles with particle size are broken.

In terms of collision frequency, hydrate-mixed particles are formed by the polymerization of several crystals, such as hydrate, and the fragmentation frequency proposed by Balakin[32] is

$$\beta_{bre} = bv^2R^{5/3} \quad (6)$$

where the crushing constant is

$$b = \frac{\rho_s E^{2/3}}{\gamma^{5/3}} \quad (7)$$

Where ρ_s is the particle density, E is the elastic modulus of the particle, γ is the crystal interface energy, v is the collision velocity, and R is the particle size before crushing. In terms of aggregation efficiency, the fluctuation of the flow leads to the generation of turbulence, and the turbulence then forms vortices. The vortices cause turbulent dissipation, and the energy will be transferred from large eddies to small eddies. The smallest vortex size is the Kolmogorov scale, and its function expression is $l = \frac{\nu^3}{\varepsilon}$. Where ν is the dynamic viscosity, and ε is the turbulent dissipation rate. Second, the shear force generated by the vortices in the region has the main influence on the aggregation of hydrates. In terms of shear collision frequency, when the hydrate particles are smaller than the Kolmogorov scale, they are in the turbulent dissipation region, and the aggregation frequency of hydrate particles is affected by the local shear stress in the vortex. Based on Clarke et al.,[33] the collision frequency is defined as

$$\beta_{agg}' = \sqrt{\frac{8\pi}{15}}\tau_v\frac{(L_i+L_j)^3}{8} \quad (8)$$

where τ_v is the local absolute velocity gradient of the flow field.

When the hydrate particles are larger than the Kolmogorov scale, they are in the inertial movement zone and move under the traction of the mainstream field. In this case, the collision frequency can be calculated by the formula proposed by Zhao,[34] as shown in 9

$$\beta_{agg}'' = 2^{3/2}\sqrt{\pi}\frac{(L_i+L_j)^3}{4}\sqrt{(u_i^2+u_j^2)^2} \quad (9)$$

where u_i^2 is the square of the average velocity of the particle.

Since hydrate is a secondary phase in Euler's two-fluid model, accounting for a small proportion, the liquid bridging force between hydrate particles can be neglected, and its coalesce efficiency is mainly van der Waals force and flow shear force. The coalesce calculation formula[35] is shown in 10

$$a = k\left(\frac{20H}{3\pi\mu R'^3\lambda}\right)^{0.242} \quad (10)$$

The deformation rate is $\lambda = \left(\frac{4\varepsilon}{15\pi\nu}\right)^{0.5}$, where H is the Hamaker constant characterizing the van der Waals force, R' is the radius of 0.5 after particle collisions have changed, k is the empirical constant 0.732, and μ is kinematic viscosity.

The capture technology of particle size after crushing is relatively complicated, and there is no way to obtain a very precise particle size distribution by certain means. In the case where the particles have a small particle distribution after crushing, only the case of crushing is considered. There are usually three sub-particle distribution functions (binary distribution, ternary distribution, and Gaussian distribution) to simplify the description of sub-particle distribution. The binary distribution is to break the large particle hydrate into two equal small hydrate particles, and the expression is

$$b(L|L') \begin{cases} 2 & L = \frac{1}{2}L' \\ 0 & L \neq \frac{1}{2}L' \end{cases} \quad (11)$$

The ternary distribution is to break the large particle hydrate into 1 small particle and 2 smaller hydrate particles, which is expressed as

$$b(L|L') \begin{cases} 1 & L' = L/2 \\ 2 & L' = L/4 \\ 0 & \text{else} \end{cases} \quad (12)$$

Gaussian distribution is a probability density function. Some researchers have shown that there is no significant difference in the distribution functions of the three sub-particles, so from the point of view of computational efficiency, the binary distribution is the most suitable. The key parameters are set in the above formula.

2.4.4. Model Verification. The experimental study of Wang[36] shows that when the critical concentration of hydrate is 35% and the critical velocity is 2 m/s, a large range of blockages will be caused in the pipeline during the transportation of hydrate. In order to study whether the pipeline spiral flow can improve the transportation capacity of hydrate in the high-concentration transportation process, the maximum concentration (30%) of hydrate in the initial concentration can be used for a numerical simulation study, and the conveying capacity of the pipeline spiral flow can be compared by the change of concentration and flow rate. In order to facilitate comparison with relevant experimental data, experimental conditions with relevant pipe spiral flow pressure drop characteristics were adopted in the simulation conditions, and specific parameters of the simulation conditions are shown in Table 3.

Based on relevant experiments,[37] the measured pressure drop was compared with the simulated pressure drop. Figure 5 shows the comparison curves of experimental values and numerical values under different conditions. Working conditions 1−3 are the flow pressure drop in the hydrate pipe with high concentration, although there are some errors; working conditions 4−8 are the normal straight pipe flow and no hydration flow; the ratio error between the numerical calculation and the experimental data is small; and the trend of change between the experimental value and the numerical simulation

https://doi.org/10.1021/acsomega.3c02549
ACS Omega 2023, 8, 26301−26316

Table 3. Simulated Condition Parameter Table

working condition	velocity V_0 (m/s)	hydrate volume fraction α (%)	with or without twisted tape
case 1	1.5	30	yes
case 2	2.0	30	yes
case 3	3.0	30	yes
case 4	1.5	30	no
case 5	2.0	30	no
case 6	3.0	30	no
case 7	2.0	0	no
case 8	2.0	0	yes
case 9	2.0	10	yes
case 10	2.0	15	yes
case 11	2.0	20	yes
case 12	2.0	25	yes

value is consistent and in good agreement, indicating that this method can simulate the hydrate slurry flow in the spiral pipe. The hydrate particle size can be described by the simulation method. It provides a theoretical basis for explaining the influence of particle size on hydrate concentration distribution.

3. RESULTS AND DISCUSSION

3.1. Stable Time of the Flow Field in the Hydrocyclone.

3.1.1. Particle Agglomeration Stable Time. After the hydrocyclone runs stably, the hydrate particle size does not change much in the hydrocyclone, and it can be considered that the flow field in the hydrocyclone has reached a stable state. In the hydrocyclone, the agglomeration behavior of the particles is caused by the mutual movement of the particles. The particle momentum determines the collision frequency, and the particles bounce or coalesce after collision and cause agglomeration. The main reason for the change of particle size is the two different agglomeration methods: dynamic agglomeration and turbulent agglomeration. The reasons for the formation of the two agglomeration methods are the dynamic agglomeration formed by the different sedimentation rates of different particles in the hydrocyclone and the turbulent agglomeration of the particles due to the inertia difference under the action of the turbulent flow in the flow field in the hydrocyclone. Turbulent agglomeration has a great influence on the separation of particles in hydrocyclones. The change of hydrate particles in the hydrocyclone is shown in Figure 6. Before 2.5 s, the size of hydrate particles changes greatly, which is due to the turbulent agglomeration of hydrate particles at the beginning. During centrifugal separation, the aggregation frequency of hydrate particles also increases. It can be seen from the figure that the mixed particles of mud−sand hydrate that have just entered the hydrocyclone have small hydrate particles, and the particles continue to swirl during the hydrocyclone process. At this time, the turbulent aggregation efficiency is improved, and the particle size of hydrate particles increases rapidly at 0−1.5 s. After reaching agglomeration equilibrium after 2.5 s, the hydrate particles reach dynamic equilibrium and do not aggregate. At this time, the hydrate particles begin to undergo dynamic agglomeration. Due to the sedimentation or floating of hydrate particles of different densities, the particle size is in dynamic equilibrium. To maintain a certain particle size and number of particles, the hydrate particles are drawn into the inner swirl zone and discharged from the overflow port, and the sand settling port discharges heavier mud sand particles or some incompletely separated mixed particles.

The average particle size of hydrate is basically unchanged at about 2.5 s, and the particle aggregation in the hydrocyclone has reached a dynamic equilibrium at this time, indicating that the stable operation time of the hydrocyclone has been reached. After entering the stabilization time, the existence of the built-in twisted tape makes the formation of hydrate particle size stable, and the fluctuation range is small. It can be seen from the figure that after entering the stable operation time, the particle size of hydrate particles in the built-in twisted tape hydrocyclone is larger than that of the basic hydrocyclone, indicating that the hydrate particles in the built-in twisted tape hydrocyclone's agglomeration behavior in the internal flow field is relatively violent, and the degree of particle aggregation is also high; second, when the number of hydrate particles is constant, the size of the hydrate particles in the built-in twisted tape hydrocyclone increases significantly, which may be due to the hydration carried in the mud sand. The collision between the material particles and the twisted tape causes the kinetic energy of the particles to be lost, part of the hydrate particles stuck in the

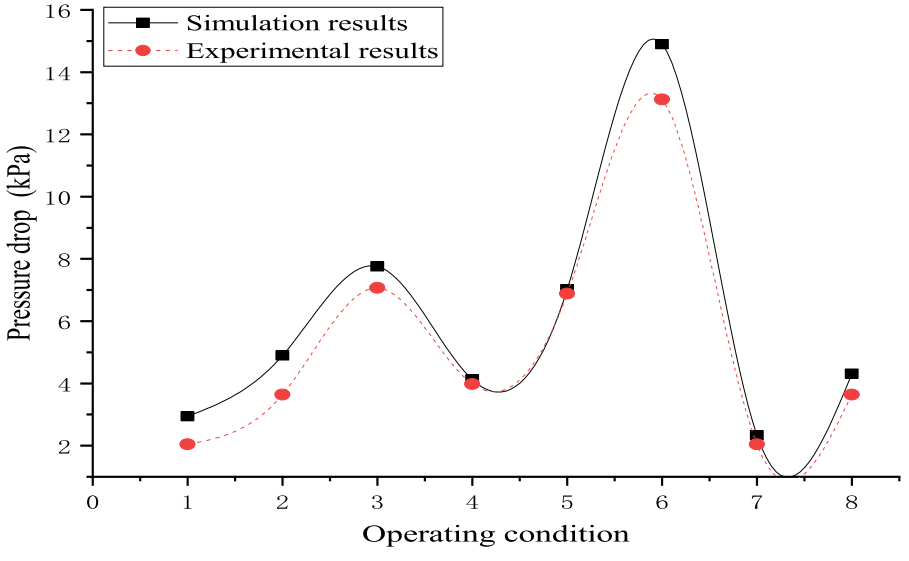

Figure 5. Pressure drop curve under different working conditions.

https://doi.org/10.1021/acsomega.3c02549
ACS Omega 2023, 8, 26301−26316

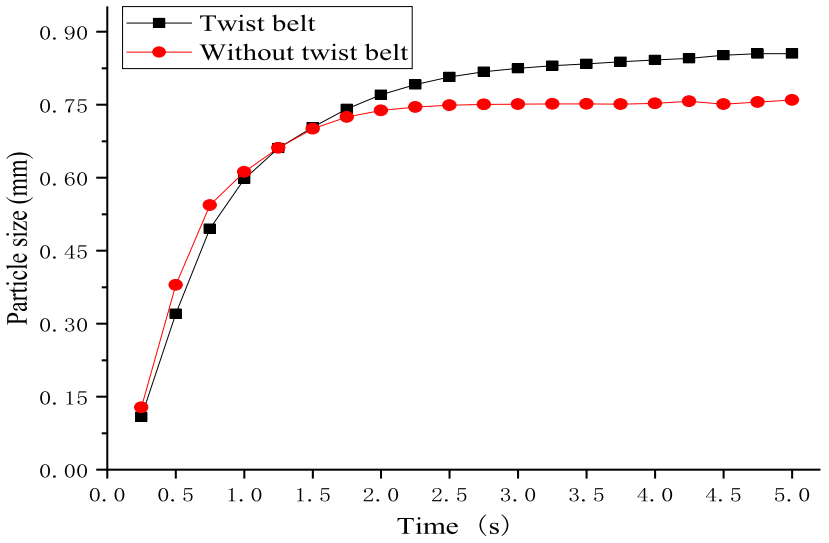

Figure 6. Average particle size versus time curve.

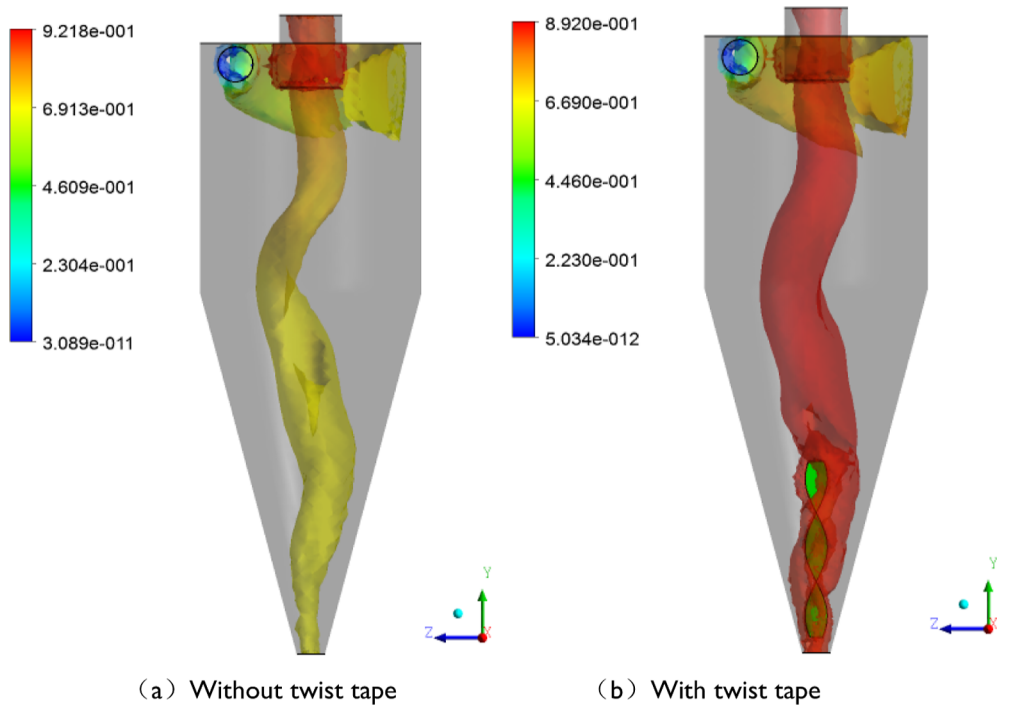

Figure 7. Cloud map of hydrate particle distribution.

mud and sand are peeled off, the number of particles increases, and more hydrate particles aggregate to form large-sized hydrates, so in the built-in twisted tape hydrocyclone, the average particle size of the inner particles is larger than that of the basic hydrocyclone.

3.1.2. Particle Agglomeration in Hydrocyclones. From Figure 7, we can see more clearly the distribution of hydrate particles in the hydrocyclone with or without the built-in twisted tape after the agglomeration behavior occurs. In the internal flow field, the volume ratio of large-particle hydrate without built-in twisted tape is significantly lower than that of the built-in twisted tape hydrocyclone. On the one hand, during the continuous collision between the hydrate-carrying sediment particles and the built-in twisted tape, the hydrates adhered to the sediment can be separated from it; at the same time, the hydrate particles colliding with the twisted tape are broken, so that the particle size and density are both broken. It is easier to be involved in the inner swirl zone. On the other hand, the built-in twisted tape improves the strength of the swirling flow and enhances the aggregation ability of the hydrate particles. The hydrate particles dispersed in the seawater quickly accumulate in the center of the hydrocyclone due to the enhancement of the internal swirling flow and the improvement of the aggregation ability. The formation of large-particle hydrates is beneficial to increasing the volume ratio of large-particle hydrates in the center of the hydrocyclone. From the cloud map of the concentration of large-particle hydrates from the grit chamber to the overflow port, it can be seen that the large-particle hydrates tend to accumulate in the center of the swirl, and their number concentration is much higher than that of conventional hydrates. The range of particle

https://doi.org/10.1021/acsomega.3c02549
ACS Omega 2023, 8, 26301−26316

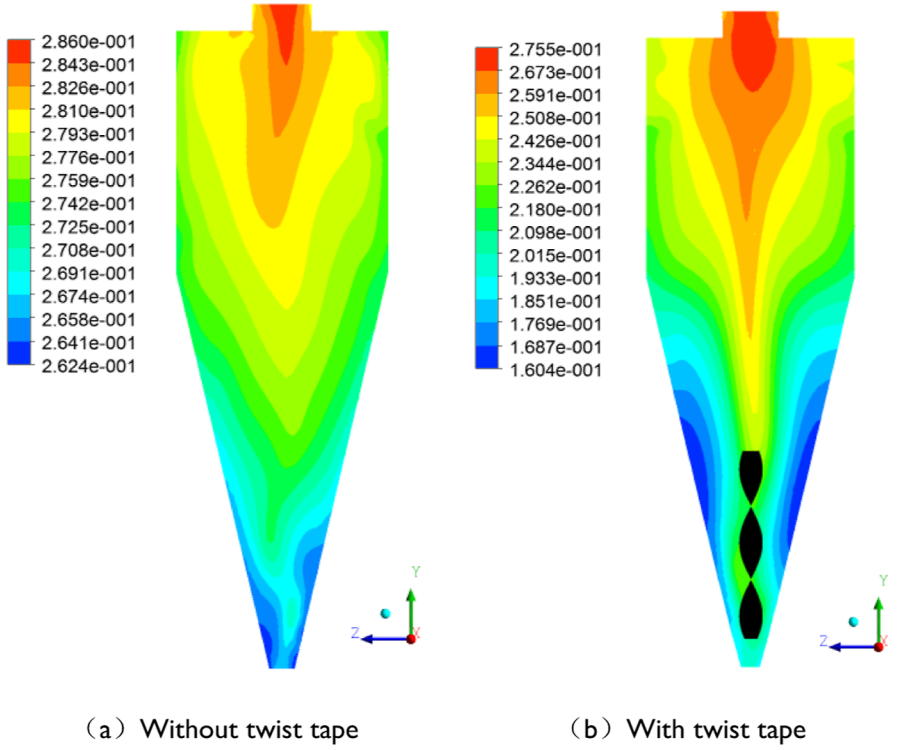

Figure 8. Cloud pattern of agglomeration and stable hydrate concentration distribution in a hydrocyclone.

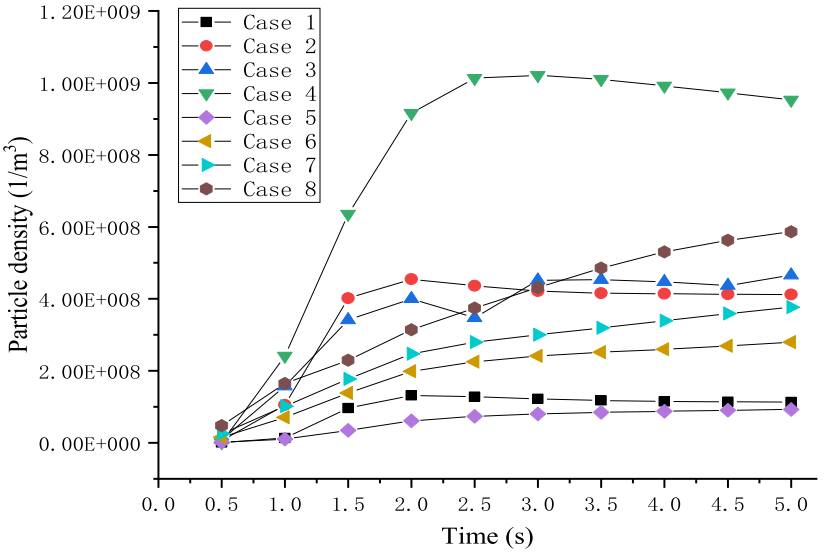

Figure 9. Curve of particle number density versus time.

hydrates aggregated in the center. The above factors are all conducive to the discharge of hydrate particles in the overflow and to improving the separation efficiency of mud and sand.

3.1.3. Particle Concentration Distribution when Stable. As shown in Figure 8 above, the distribution of hydrate particles in the hydrocyclone after the particle agglomeration degree is stabilized. In the basic hydrocyclone, the stabilized hydrate particles are mainly distributed in the overflow port, but some hydrate particles are also distributed in the short-circuit flow area, which causes the hydrate particles to be unable to be discharged from the overflow port in time; the "tail swing" phenomenon occurs in the cone section at the lower end of the hydrocyclone, which will cause the mud and sand particles to entrain hydrate particles again, both of which are not conducive to the improvement of the separation efficiency. In the built-in twisted tape hydrocyclone, the hydrate particles are mainly concentrated near the overflow port of the inner hydrocyclone zone. The built-in twisted tape enhances the aggregation ability of hydrate particles, and at the same time, the hydrate distribution concentration on the wall of the lower cone section is enhanced. The hydrate accumulation degree is high from the upper part of the built-in twisted tape to the overflow outlet, the hydrate is stably distributed in the inner hydrocyclone region, and the hydrate particle concentration is distributed in an "inverted cone" shape in the hydrocyclone. The high degree of hydrate aggregation in the inner swirl region and the absence of

https://doi.org/10.1021/acsomega.3c02549
ACS Omega 2023, 8, 26301−26316

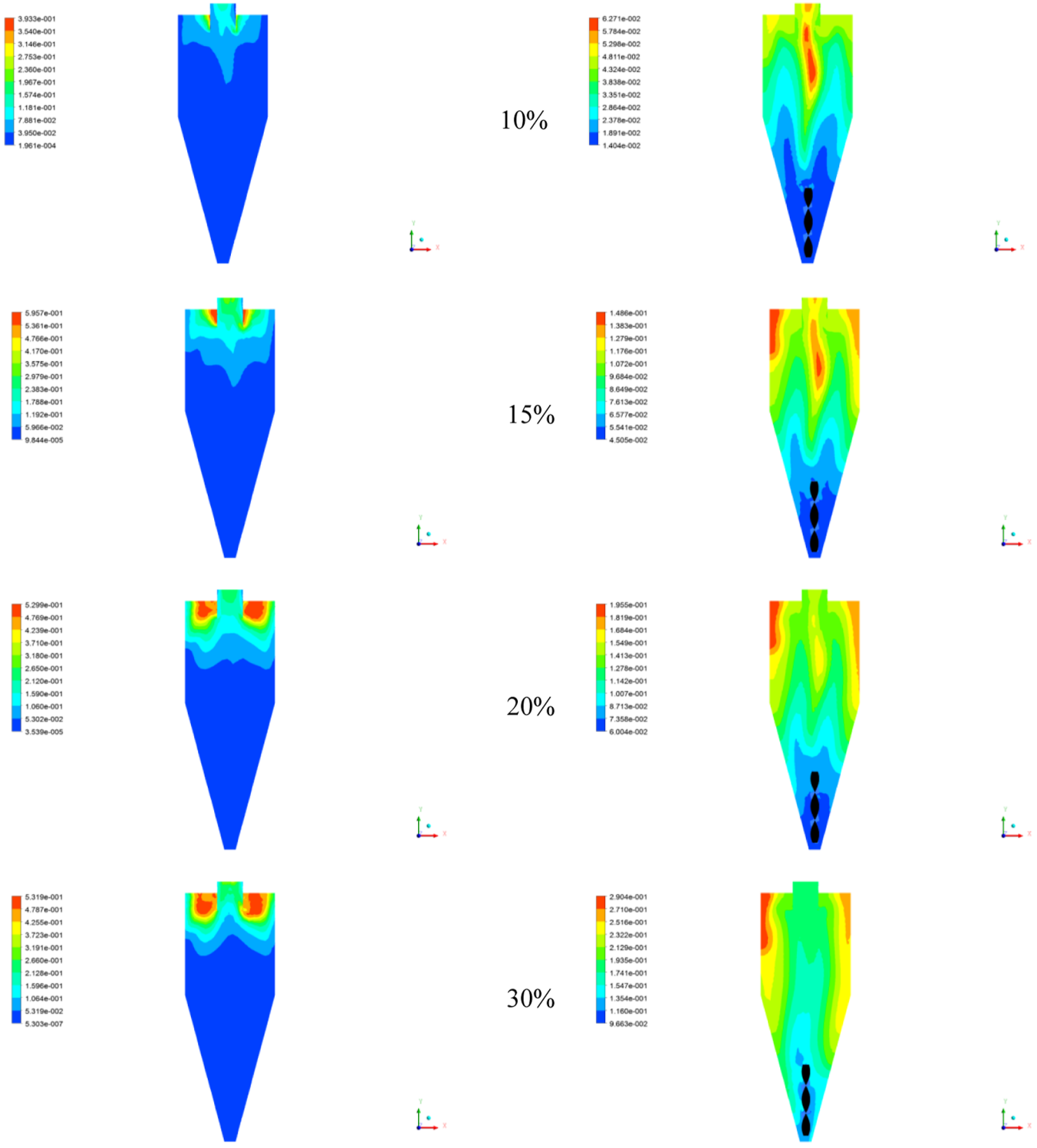

Figure 10. Cloud map of hydrate particle distribution at different initial concentrations.

secondary eddy currents caused by the phenomenon of "swing tail" are all beneficial to the improvement of the separation efficiency of mud and sand particles by the built-in twisted tape hydrocyclone.

3.2. Effect of Concentration on Separation Efficiency. In the built-in twisted tape hydrocyclone, changing the initial concentration of hydrate has an impact on the particle aggregation behavior. According to the different initial hydrate concentration conditions of working conditions 1−8, the influence of the hydrate particle agglomeration behavior and concentration distribution on the separation efficiency of the built-in twisted tape hydrocyclone was explained, and the results were compared with those of the basic hydrocyclone.

3.2.1. Particle Agglomeration Stable Time. Figure 9 shows the variation law of the number and concentration of hydrate particles with time. From 0.5 to 2 s, the number of hydrate particles increases sharply, mainly from the continuous separation of hydrate particles from mud and sand and the

https://doi.org/10.1021/acsomega.3c02549
ACS Omega 2023, 8, 26301−26316

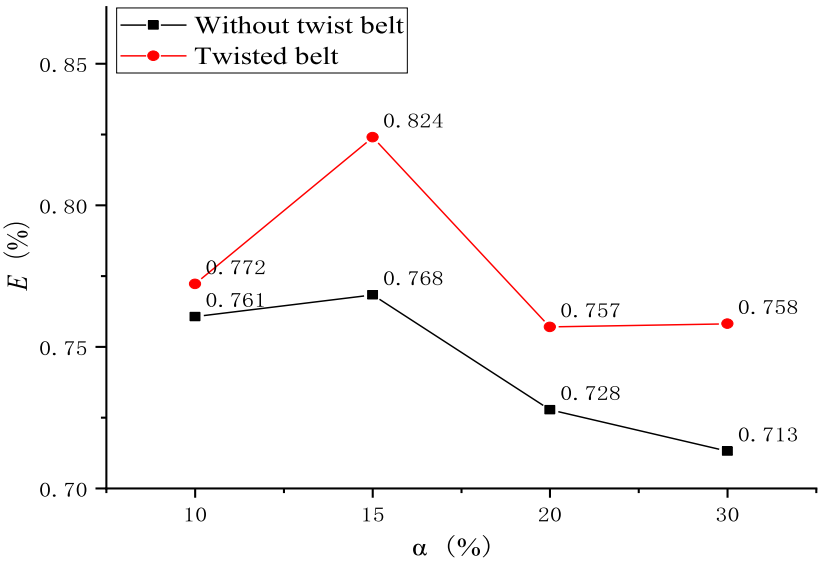

Figure 11. Effect of initial hydrate concentration on separation efficiency.

occurrence of hydrate particles. The agglomeration of the built-in twisted tape hydrocyclone and the base hydrocyclone significantly increased the number of particles. The number of hydrate particles with built-in twisted tape hydrocyclones increases with the increase of initial hydrate concentration in working conditions 1−4. Under the same initial concentration conditions, comparing the number of hydrate particles in conditions 4 and 8, the number of particles in the built-in twisted tape hydrocyclone is significantly higher than that in the basic hydrocyclone, which is the main reason for this phenomenon. The reason is that the built-in twisted tape enhances the swirl strength and increases the tangential velocity, the hydrate particles stuck in the mud and sand are hit by the built-in twisted tape, and the hydrate and the mud−sand particles are more fully separated; second, the built-in twisted tape enhances the internal flow field. It reduces the secondary eddy current in the cone section and avoids the "secondary mixing" of hydrate particles and mud sand particles. The high degree of aggregation of hydrate particles and the large number of hydrate particles are beneficial to the improvement of hydrate separation efficiency. After entering the stable operation state of the hydrocyclone for 2.5 s, the fluctuation range of the particle number of the built-in twisted tape hydrocyclone is smaller than that of the basic hydrocyclone, which can further illustrate that the built-in twisted tape helps to improve the flow field in the hydrocyclone and the stabilization of particles after agglomeration.

3.2.2. Hydrate Particle Concentration Distribution. After the hydrocyclone runs stably, it can be seen from the cloud diagram of the concentration distribution of hydrate particles in Figure 10 that in the conventional hydrocyclone, the hydrate particles increase with the concentration, and the hydrate accumulated in the short-circuit flow area the concentration also increases, and it is difficult for the hydrate particles to be involved in the inner swirling flow area. At this time, a large amount of hydrate deposited in the short-circuit flow area cannot be removed in time, which will cause it to mix with the mud sand particles, resulting in the hydrocyclone on the mud sand separation efficiency. For the built-in twisted tape hydrocyclone, the twisted tape increases the aggregation ability and swirl strength of hydrate so that the hydrate particles are drawn into the inner swirl zone, showing that the hydrate particles mainly gather in the overflow. Near the mouth and the location of the internal swirl zone. With the increase of the initial hydrate concentration in the built-in twisted tape hydrocyclone, the contact between the hydrate particles becomes more frequent, and the turbulent agglomeration of the hydrate particles in the hydrocyclone will further aggravate the agglomeration between the hydrate particles. After a large amount of hydrate agglomeration, the particle size of the hydrate increases, and the specific gravity also increases, and at this time, it is enhanced by the tangential velocity of the built-in twisted tape. After the agglomeration is formed, the centrifugal radius of the large-particle hydrate will increase, and the hydrate particles are thrown to the wall, resulting in a high hydrate concentration distribution at the wall. It can be seen from the cloud map that the concentration of hydrate particles is in the range of 10−20%, the aggregation effect of hydrate particles in the inner swirl zone is better, and it is not easy to be thrown to the wall of the hydrocyclone. It is beneficial to the improvement of the separation efficiency of mud and sand by the hydrocyclone.

3.2.3. Separation Efficiency. As shown in Figure 11, under different hydrate concentrations, the comparison curves of the mud−sand separation efficiency between the built-in twisted tape and the conventional hydrocyclone were obtained. It can be seen from the figure that when the initial hydrate concentration of the two hydrocyclones is 15%, the separation efficiency of mud and sand is the highest, and the separation efficiency decreases as the concentration increases. When the hydrate inlet concentration is too high, the volume proportion of hydrate particles also increases, the number of hydrate particles increases, and the hydrate particles are more likely to float in the short-circuit flow area. In the conventional hydrocyclone, the concentration of hydrate particles is too high, the centrifugal force generated at a certain tangential velocity is not enough to separate the hydrate particles from the mud sand, and it is difficult for the hydrate particles to be directly involved in the inner swirl zone, which intensifies the hydration. Then, the hydrate is carried by the mud and settled to the sand settling port for discharge, which reduces the separation efficiency of mud and sand. However, when the initial concentration of hydrate is relatively high, the built-in twisted zone has the characteristics of enhancing the swirling flow and preventing the direct settlement

https://doi.org/10.1021/acsomega.3c02549
ACS Omega 2023, 8, 26301−26316

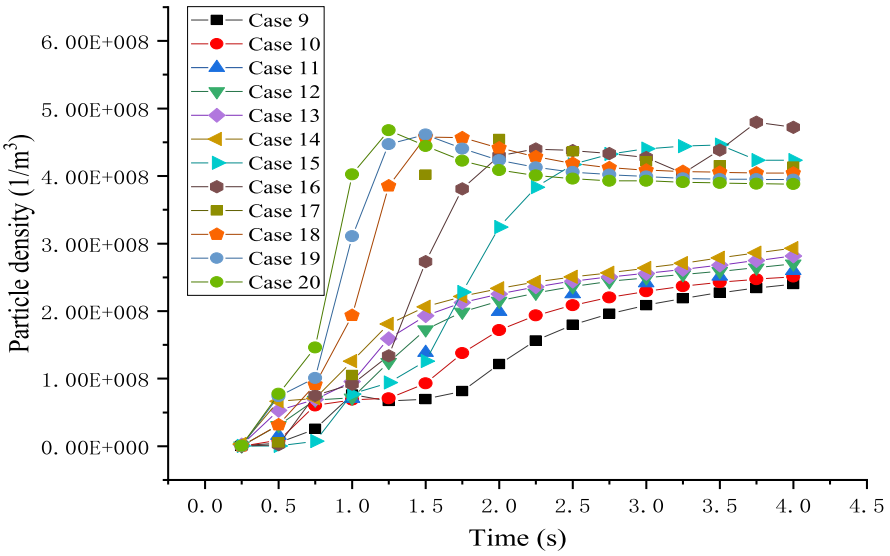

Figure 12. Curve of particle number density versus time.

of mud and sand. When the inlet flow rate is the same as that of the basic hydrocyclone, the swirl direction of the built-in twisted tape is the same as that of the hydrocyclone, which can increase the tangential velocity of the internal flow field and increase the centrifugal force; the twisted tape is prevented, and the mixed particles of hydrate, mud, and sand that are not completely separated can be prevented from being directly discharged and settled from the sand chamber. The kinetic energy makes the hydrate particles separate from it, and due to the action of buoyancy, the hydrate re-enters the inner swirling flow area, and the separation efficiency of mud and sand is improved. As the initial concentration increases, the separation efficiency of the built-in twisted tape hydrocyclone is still higher than that of the basic hydrocyclone.

3.3. Effect of Speed on Separation Efficiency. *3.3.1. Particle Agglomeration Behavior.* As shown in Figure 12, with the increase of the inlet flow velocity, the stable time of particle aggregation in the hydrocyclone is earlier, indicating that the inlet flow velocity increases, the turbulence intensity increases, the aggregation effect of turbulence is aggravated, the hydrate particles increase with the flow velocity, and reunion quickens. It can be seen from Figure 12 that the slope of the hydrate particle number concentration curve of the basic hydrocyclone is relatively large in working conditions 15−20, and the hydrate particle number rises faster at this time, indicating that the hydrate particles are in the conventional hydraulic system. Due to the increase of the flow velocity in the hydrocyclone, the turbulent effect is more severe, the number of hydrate particles increases significantly at this time, and the earlier the stabilization time of the hydrocyclone is. However, with the passage of time, the number of hydrate particles shows a downward trend, and the number of particles fluctuates repeatedly. At this time, the reason for the decrease and fluctuation of the number of particles may be due to the formation of secondary eddy currents in the cone section of the hydrocyclone, which makes the hydrate particles and the mud sand. Particle blending, the hydrate particles entrained by the mud and sand particles are discharged from the sand settling port, thus reducing the number density of hydrate particles. The faster the flow rate, the more serious the mixing of mud, sand, and hydrate, and the greater the decrease in the number of hydrate particles. Therefore, the increase of the flow rate causes the instability of the flow field in the basic hydrocyclone. The built-in twisted tape can alleviate the fluctuation of the flow field in the hydrocyclone caused by the change of the flow rate. It can be seen from Figures 9 and 10 that the number density of the particles in the built-in twisted tape hydrocyclone increases slowly, the flow rate has little effect on the particle density, and the particle number density shows a steady upward trend with time. It shows that the built-in twisted tape hydrocyclone can enhance the stability of the internal flow field. After 2.5 s, the built-in twisted tape hydrocyclone entered a stable operation state, and at the same time, the number density of hydrate particles showed an upward trend, which indicates that the built-in twisted tape separated a small amount of hydrate particles carried in mud and sand for a second time, which improved the hydration rate. The number of solid particles, the stable flow field, and the increase in the number of hydrate particles are beneficial to the improvement of the separation efficiency of mud and sand.

It can be seen from Figure 13 that when the 2.5 s operating condition reaches stability, under the same operating conditions

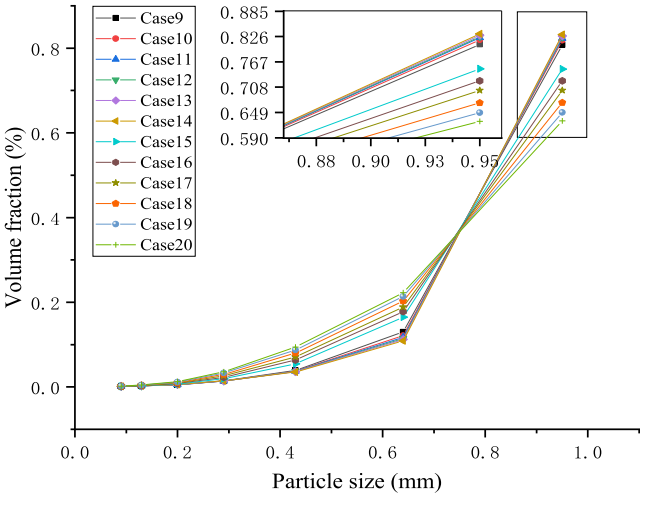

Figure 13. Hydrate particle size proportion at different inlet velocities.

https://doi.org/10.1021/acsomega.3c02549
ACS Omega 2023, 8, 26301−26316

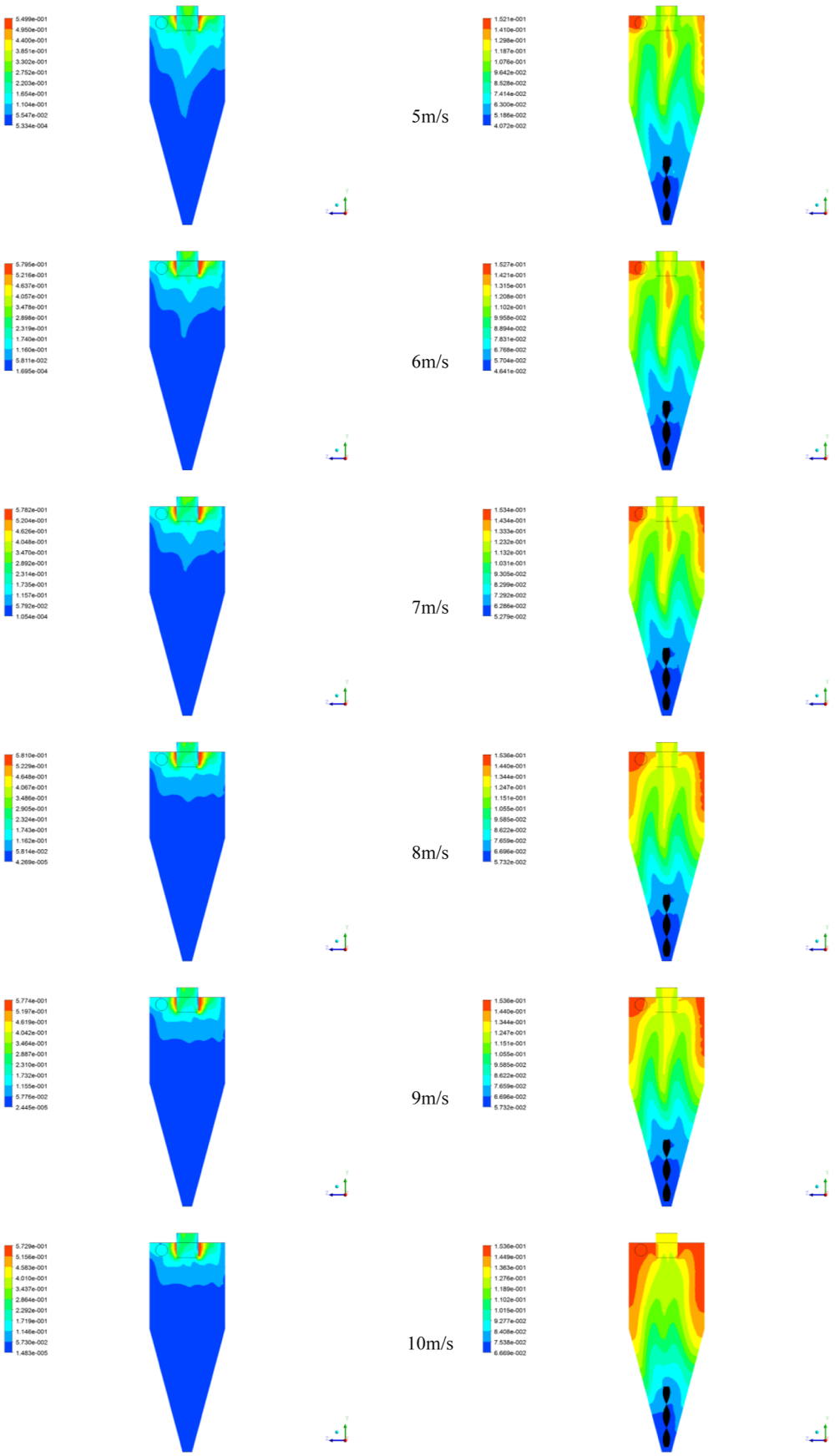

Figure 14. Cloud map of hydrate particle distribution at different inlet velocities.

https://doi.org/10.1021/acsomega.3c02549
ACS Omega 2023, 8, 26301−26316

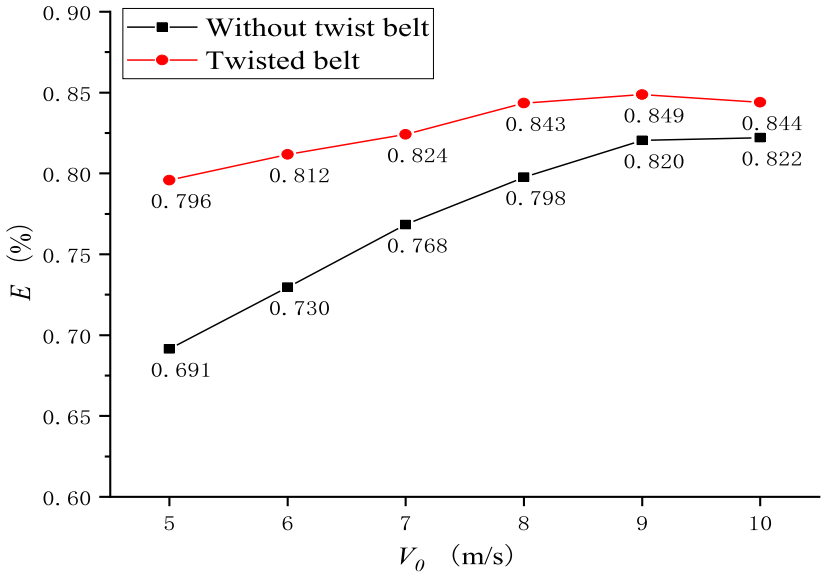

Figure 15. Separation efficiency curves at different inlet velocities.

of the two hydrocyclones, the change of the inlet flow rate has a more obvious effect on the particle size of the hydrate particles after agglomeration in the built-in twisted tape hydrocyclone. The inlet velocity leads to the accelerated movement of the particles to be separated, and the turbulent effect of the particles in the flow field is intensified. In addition, the flow field in the built-in twisted tape hydrocyclone is stable, and the higher the degree of particle aggregation, the larger the volume of large particles of hydrate. On the other hand, the basic hydrocyclone has severe fluctuations in the flow field due to the increase of the flow rate, the shear force on the hydrate particles increases at this time, and it is difficult to form large hydrate particles, so the particle size of the hydrate particles is small.

As shown in Figure 10, when the inlet flow rate is 5−10 m/s, the corresponding particle size ratio curves are obtained. It can be seen from the figure that the particle size accounts for the largest proportion when the particle size is 0.9 mm. The proportion of the particle size in the range of 0.15−0.45 mm is the lowest, indicating that the particles in the hydrate particle hydrocyclone are agglomerated due to the hydrocyclone, showing a trend of increasing particle size. Comparing the proportion of hydrates with a maximum particle size of 0.95 mm, it can be found that the larger the flow rate in the conventional hydrocyclone, the lower the proportion of large particles of hydrate decreases, while in the built-in twisted tape hydrocyclone, the greater the flow rate, the higher the proportion of large particle hydrates. It shows that with the increase of the flow velocity in the conventional hydrocyclone, the internal flow field fluctuates more violently. At this time, the shear force on the hydrate particles also increases, and the particle crushing energy is greater than the aggregation capacity. The twisted ribbon enhances the stability of the flow field in the hydrocyclone. The increase of the flow velocity increases the contact frequency of the hydrate particles, the turbulent coalescence effect is strong, and the aggregation capacity of the hydrate particles is greater than the breaking capacity, so at high flow velocity, the 0.95 mm large particle hydrate is in the built-in twisted tape hydrocyclone. The large proportion of large-particle hydrate is beneficial to the aggregation of hydrate particles in the inner hydrocyclone zone and the improvement of mud−sand separation efficiency. Although the proportion of large-particle hydrate in the built-in twisted tape hydrocyclone is significantly higher than that in the basic hydrocyclone, the change in flow rate has little effect on the proportion of large-grained hydrate in the built-in twisted tape hydrocyclone.

3.3.2. Hydrate Particle Concentration Distribution. After the hydrocyclone runs stably, the distribution of hydrate particles in the hydrocyclone at different flow rates needs understanding. As shown in Figure 14, when the inlet flow rate is 5−6 m/s, the centrifugal force generated by the hydrate in the basic hydrocyclone is too small, and when the hydrate particles are not completely separated from the mud and sand, the hydrate particles will not be completely separated. The concentration in the hydrocyclone is low; in addition, the tangential velocity generated by the low inlet flow rate is very small, which is not enough to directly entrain the hydrate particles into the inner hydrocyclone zone, and the hydrate particles are subjected to buoyancy and float and deposit in the overflow the nozzle, the short-circuit flow area, and the internal swirl area cannot make the hydrate particles gather as soon as possible. These two factors are not conducive to the improvement of the separation efficiency of mud and sand. For the built-in twisted tape hydrocyclone, due to the existence of twisted tapes, some of the mixed particles of mud−sand hydrate that are not completely separated swirly descend along the wall of the twisted tape and at the same time increase the collision frequency of hydrate and sand particles on the wall of the twisted tape, forcing the hydrate particles to separate from the crushed mud and sand, and the hydrate concentration in the inner swirl zone increases. As the inlet flow rate increases, the twisted tape rotation is the same as that of the hydrocyclone, and the swirl strength increases, forcing more hydrate particles stuck in the mud and sand to be separated out for the second time. The flow rate increases, and with the built-in twisted tape hydrocyclone, the hydrate particle concentration in the flow vessel also increases. However, if the flow velocity increases too much, most of the agglomerated hydrate particles are distributed in the inner swirl zone in the center of the built-in twisted tape, and the other part is thrown to the outer swirl zone due to the increase of the tangential velocity. The more particles, the more the inlet flow rate continues to increase at this time, which is not conducive to the improvement of the separation efficiency of mud and sand.

https://doi.org/10.1021/acsomega.3c02549
ACS Omega 2023, 8, 26301−26316

Compared with the basic hydrocyclone, the hydrate particles in the built-in twisted tape hydrocyclone are easier to gather in the inner hydrocyclone area at low flow rates and will not accumulate in the short-circuit flow area. At an inlet flow rate of 6−8 m/s, the distribution effect of hydrate particles in the hydrocyclone is the best, and this flow rate is conducive to the improvement of the mud−sand separation efficiency of the built-in twisted tape hydrocyclone.

3.3.3. Separation Efficiency. According to the calculation results of the separation efficiency, when the hydrate concentration is 15%, the separation efficiency is the highest, so 15% is selected as the initial concentration of the hydrocyclone, and the optimal pairing of the hydrocyclone is studied by changing the flow rate of the feed port. As shown in the separation efficiency curves of different velocities in Figure 15, when the flow velocity is greater than 8 m/s, increasing the flow velocity cannot significantly improve the silt separation efficiency of the hydrocyclone. Through the analysis of the hydrate particle number and concentration distribution, it can be found that increasing the flow rate makes it easier to strip the hydrate particles stuck in the mud sand, increase the number of hydrate particles, and accelerate the sedimentation of the mud sand. However, with the increase of the swirl intensity, the particle aggregation degree increases, and the large particles of hydrate will be thrown into the short-circuit flow area or the outer swirl area. Separation efficiency. In conclusion, under the premise of ensuring separation efficiency and safe operation, 8 m/s was selected as the inlet flow rate of the built-in twisted tape hydrocyclone.

4. CONCLUSIONS

(1) The sand removal effect of the built-in twisted tape hydrocyclone is better than that of a basic hydrocyclone. The built-in twisted tape not only eliminates the obstruction of the air column to the discharge of mud and sand from the sand chamber, but it also can enhance the swirl strength and improve the resistance to mud and sand. At the same time, the stability of the swirl flow is enhanced. After the incompletely separated natural gas hydrate mud sand particles collide with the twisted tape, the kinetic energy of the particles is lost, and it can force the hydrate to be stripped from the mud sand particles. After the transformation, the incompletely separated particles re-entered the outer hydrocyclone area for secondary separation, and they can form a peak of hydrate content at the overflow outlet, while the basic hydrocyclone fails to show a large number of hydrate particles aggregated at the overflow outlet. The phenomenon shows that the built-in twisted tape helps improve separation efficiency.

(2) With the increase of the initial concentration of hydrate, the number of hydrate particles in the built-in twisted tape hydrocyclone increases, and the contact frequency between hydrate particles will increase, which can intensify the aggregation of hydrate and increase the particle size of hydrate. The tangential velocity increases after the built-in twisted tape enhances the swirl flow, and the hydrate particles are thrown into the outer swirl zone. Considering the above factors, the optimum concentration condition is that the volume of mud and sand accounts for 25%, and the initial concentration of hydrate is 15%.

(3) When the initial concentration of hydrate particles is 15%, the inlet flow velocity improves the separation efficiency of the hydrocyclone. When the inlet velocity is higher than 8 m/s, the improvement of the separation efficiency is no longer obvious. The hydrocyclone increases when the inlet flow increases, and the time of stable operation of the hydrocyclone is also earlier. Excessive inlet flow will inevitably lead to an unstable flow field inside the hydrocyclone. The built-in twisted tape will form a buffer against sudden flow velocity changes and enhance the stability of the internal flow field. If the centrifugal force required for separation cannot be achieved, the tangential velocity formed by the too low flow rate. The unseparated hydrate particles will be carried by the mud and sand and will directly settle. The strength of the swirl flow makes the stripped hydrate more likely to be involved in the inner swirl zone, which improves the separation efficiency of mud and sand. When the two factors of operation stability and separation efficiency are considered, the inlet flow rate of 8 m/s is finally selected.

■ ASSOCIATED CONTENT

Data Availability Statement

The data presented in this study are available on request from the corresponding author.

■ AUTHOR INFORMATION

Corresponding Author

Shuli Wang − *School of Energy, Quanzhou Vocational and Technical University, Quanzhou, Fujian 362268, China*; Email: wsl@cczu.edu.cn

Authors

Yongchao Rao − *Jiangsu Key Laboratory of Oil−Gas Storage and Transportation Technology, Changzhou University, Changzhou, Jiangsu 213164, China; School of Petroleum and Gas Engineering, School of Energy, Changzhou University, Changzhou, Jiangsu 213164, China*; orcid.org/0000-0003-4933-7758

Yong Hu − *Jiangsu Key Laboratory of Oil−Gas Storage and Transportation Technology, Changzhou University, Changzhou, Jiangsu 213164, China; School of Petroleum and Gas Engineering, School of Energy, Changzhou University, Changzhou, Jiangsu 213164, China*

Shuhua Zhao − *Jiangsu Key Laboratory of Oil−Gas Storage and Transportation Technology, Changzhou University, Changzhou, Jiangsu 213164, China; School of Petroleum and Gas Engineering, School of Energy, Changzhou University, Changzhou, Jiangsu 213164, China*

Shidong Zhou − *Jiangsu Key Laboratory of Oil−Gas Storage and Transportation Technology, Changzhou University, Changzhou, Jiangsu 213164, China; School of Petroleum and Gas Engineering, School of Energy, Changzhou University, Changzhou, Jiangsu 213164, China*; orcid.org/0000-0001-8468-1226

Complete contact information is available at: https://pubs.acs.org/10.1021/acsomega.3c02549

Notes

The authors declare no competing financial interest.

https://doi.org/10.1021/acsomega.3c02549
ACS Omega 2023, 8, 26301−26316

■ ACKNOWLEDGMENTS

This work was supported by the National Nature Science Foundation of China (no. 51574045 and 51974037), the CNPC Innovation Foundation (no. 2020D-5007-0211), the Project of Emission Peak and Carbon Neutrality of Jiangsu Province, China (no. BE2022001-5), the General Project of Natural Science Research in Jiangsu Universities (no. 22KJB440002), the Quanzhou Science and Technology Planning Project (no. 2022N045), the Vice General Project of Science and Technology of Jiangsu Province (no. FZ20211199), the Open Project of Collaborative Innovation Center for Clean Energy Application Technology(Quanzhou Vocational and Technical University) (no. QJNY22-06), and the Opening Fund of Jiangsu Key Laboratory of Oil-gas Storage and Transportation Technology(Changzhou University) (no. CDYQCY202105).

■ REFERENCES

(1) Sloan, E. D.; Koh, C. A. *Clathrate Hydrates of Natural Gases*; Marcel Dekker, CRC Press: New York and Basel, 2008; pp 2−5.
(2) Zhou, S. W.; Chen, W.; Li, Q. P. Green technology of solid fluidization of gas hydrate in deep water and shallow layer. *China offshore oil and gas* **2014**, *26*, 1−7.
(3) Kelland, M. A. History of the development of low dosage hydrate inhibitors. *Energy Fuels* **2006**, *20*, 825−847.
(4) Sloan, E. D.; Koh, C. A.; Sum, A. K. *Natural Gas Hydrates in Flow Assurance*; Elsevier Gulf Professional Publishing, 2010; pp 1−10.
(5) Shi, B.-H.; Gong, J.; Sun, C.-Y.; Zhao, J.-K.; Ding, Y.; Chen, G.-J. An inward and outward natural gas hydrates growth shell model considering intrinsic kinetics, mass and heat transfer. *Chem. Eng. J.* **2011**, *171*, 1308−1316.
(6) Rao, Y.; Sun, Y.; Wang, S.; Ge, H.; Ding, B.; Yang, M. Investigation on gas hydrate formation properties in a spiral flow using a flow loop. *Int. J. Oil, Gas Coal Technol.* **2020**, *25*, 292−318.
(7) Xu, Y. V.; Tang, B.; Song, X. F. Simulation and analysis of internal flow field of hydrocyclone and PIV verification. *J. East China Univ. Sci. Technol.* **2013**, *39*, 1−7.
(8) Baker, R.; Schook, R. The Multiphase Separation and Multiphase Pump Technologies. *Conference of Multiphase Separation and New Technologies*, 2005; pp 125−136.
(9) Westra, R. W. Compact inline water separation at ATP oil&gas (UK) Ltd Kilmar Platform-Southern North Sea. *Tekna Produced Water Conference*, **2014**; pp. 1258-1266.
(10) Zhao, L. X.; Li, Y. Q.; Xu, B. R. Influence of inner cone diameter on degassing and sand removal integrated cyclone. *Oil Field Equip.* **2014**, *10*, 31−34.
(11) Gomez, C.; Caldentey, J.; Wang, S. B.; Gomez, L.; Mohan, R.; Shoham, O. Oil/Water Separation in Liquid/Liquid Hydrocyclones (LLHC): Part 1 - Experimental Investigation. *SPE J.* **2002**, *7*, 353−372.
(12) Shang, X. F.; Ma, W. Y.; Wang, Z. J. Optimization and Experimental Study of slotted Hydrocyclone Structure Based on Orthogonality. *Fluid Mach.* **2005**, *35*, 105.
(13) Zhao, L. X.; Jiang, M. H.; Xu, B. R.; Zhu, B. J. Development of a new type highefficient inner-cone hydrocyclone. *Chem. Eng. Res. Des.* **2012**, *90*, 2129−2134.
(14) Zhao, L. X.; Han, L. Y.; Zheng, G. X. Structural Simulation and Analysisof Conical Hydrocyclone with Simultaneous Outflow. *Fluid Mach.* **2013**, *41*, 19−24.
(15) Chen, H.; Wu, W. U.; Lv, B.; Chen, J. W.; Fu, L. Q.; Gang, Y. Purification of Marine natural gas hydrate slurry by double-cone inner cone hydrocyclone. *J. Process Eng.* **2018**, *18*, 491−495.
(16) Qiu, S. Z.; Wang, G. R.; Zhou, S. W. Structure design and optimizationof gas hydrate in situ Purification Separator. *China Offshore Oil Gas* **2019**, *31*, 125−131.
(17) Liu, Y.; Wang, Z. B. Research progress on Influencing Factors of Hydrocyclone Separation Efficiency. *Fluid Mach.* **2016**, *44*, 39−42.
(18) Rao, Y.; Wang, S.; Li, L. Numerical Simulation of the Flow Pattern of Spiral Annular Flow with a Guide Strip by Spiral On-Way. *ACS Omega* **2022**, *7*, 31961−31973.
(19) Rao, Y. C.; Liu, Z. H.; Wang, S. L.; Li, L. J. Experimental Study on Hydrate Safe Flow in Pipelines under a Swirl Flow System. *ACS Omega* **2022**, *7*, 16629−16643.
(20) Rao, Y. C.; Liu, Z. H.; Wang, S. L.; Li, L. J. Numerical Simulation on the Flow Pattern of a Gas−Liquid Two-Phase Swirl Flow. *ACS Omega* **2022**, *7*, 2679−2689.
(21) Lafond, P. G.; Sloan, E. D.; Koh, C. A. Modeling Particle Jamming as a Hydrate Plugging Mechanism. *Proceedings of the 8th International Conference on Gas Hydrates*, 2014; pp 390−399.
(22) Majid, A.; Vijayamohan, P.; Chaudhari, P. Understanding gas hydrate growth in partially dispersed and water continuous systems from flow loop tests. *Offshore Technology Conference*, 2015; pp 12−19.
(23) Yongchao, R.; Shuli, W.; Shidong, Z.; Entian, L.; Wenming, L. Experimental research on velocity distribution and attenuation characteristic of spiral flow by LDV[J]. *J. Fluids Eng.* **2014**, *136*, 011104.
(24) Wang, S. L.; Ding, B. Y.; Rao, Y. C.; Chen, F. Study on the influence of coconut oil on flow pattern and pressure drop of two-phase swirl flow. *RSC Adv.* **2019**, *9*, 32644−32655.
(25) Ding, L.; Shi, B. H.; Lv, X. F.; Liu, Y.; Wu, H.; Wang, W.; Gong, J. Hydrate Formation and Plugging Mechanisms in Different Gas−Liquid Flow Patterns. *Ind. Eng. Chem. Res.* **2017**, *56*, 4173−4184.
(26) Lv, B. *Numerical Simulation of Submarine Multiphase Separation of Natural Gas Hydrate Based on Hydrocyclone*; Southwest Petroleum University, 2017; pp 25−36.
(27) Bakker, A.; Slack, M.; Cokljat, D.; Vasquez, S. A.; Montante, G. Reynolds-Stress Model for Eulerian multiphase. *Prog. Comput. Fluid Dyn.* **2006**, *6*, 168−178.
(28) Wen, C. Y.; Yu, Y. H. Mechanics of fluidization. *Chem. Eng. Prog., Symp. Ser.* **1966**, *162*, 100−110.
(29) Coleman, H. W.; Hodge, B. K.; Taylor, R. P. A Reevaluation of Schlichting's Surface Roughness Experiment. *J. Fluids Eng.* **1984**, *106*, 60−65.
(30) Hounslow, M. J.; Ryall, R. L.; Marshall, V. R. A Discretized Population Balance for Nucleation, Growth, and Aggregation. *AIChE J.* **1988**, *34*, 1821−1832.
(31) Nopens, I.; Nere, N.; Vanrolleghem, P.; Ramkrishna, D. Solving the inverse problem for aggregationin activated sludge flocculation using a population balance framework. *Water Sci. Technol.* **2007**, *56*, 95−103.
(32) Balakin, B. V.; Hoffmann, A. C.; Kosinski, P. Population Balance Model for Nucleation, Growth, Aggregation, and Breakage of Hydrate Particles in Turbulent Flow. *AIChE J.* **2010**, *56*, 2052−2062.
(33) Clarke, M. A.; Bishnoi, P. Determination of the intrinsic rate c-onstant and activation Energy of CO2 gas hydratedecompositio-n using in-situ particle size analysis. *Chem. Eng. Sci.* **2004**, *59*, 2983−2993.
(34) Zhao, P. F.; Wang, W. C.; Li, Y. X. Numerical model of hydr-ate sluryflow in pipeline. *Oil Gas Storage Transp.* **2016**, *35*, 272−277.
(35) Higashitani, K.; Yamauchi, K.; Matsuno, Y.; Hosokawa, G. T-u-rbulent Coagulation of Particles Dispersed in a Viscous Fluid. *Chem. Eng. Jpn.* **1983**, *16*, 299−304.
(36) Wang, W. C.; Chen, P.; Li, Y. X.; et al. Flow and deposition characteristics of natural gas hydrate in pipelines. *Nat. Gas Ind.* **2014**, *34*, 99−104.
(37) Li, Z. Flocculation kinetics of activated sludge based on population equilibrium, Doctoral thesis, Chongqing University, Chongqing, 2014.

https://doi.org/10.1021/acsomega.3c02549
ACS Omega 2023, 8, 26301−26316